

λ -GELU: Learning Gating Hardness for Controlled ReLU-ization in Deep Networks

Cristian Pérez-Corral*

Universitat Politècnica de València
Valencia, Spain
cpercor@upv.es

Alberto Fernández-Hernández

Universitat Politècnica de València
Valencia, Spain
a.fernandez@upv.es

Jose I. Mestre

Universitat Jaume I
Castelló de la Plana, Spain
jmiravet@uji.es

Manuel F. Dolz

Universitat Jaume I
Castelló de la Plana, Spain
dolzm@uji.es

Enrique S. Quintana-Ortí

Universitat Politècnica de València
Valencia, Spain
quintana@disca.upv.es

Abstract—Gaussian Error Linear Unit (GELU) is a widely used smooth alternative to Rectified Linear Unit (ReLU), yet many deployment, compression, and analysis toolchains are most naturally expressed for piecewise-linear (ReLU-type) networks. We study a hardness-parameterized formulation of GELU, $f(x; \lambda) = x \Phi(\lambda x)$, where Φ is the Gaussian Cumulative Distribution Function (CDF) and $\lambda \in [1, \infty)$ controls gate sharpness, with the goal of turning smooth gated training into a controlled path toward ReLU-compatible models. Learning λ is non-trivial: naive updates yield unstable dynamics and effective gradient attenuation, so we introduce a constrained reparameterization and an optimizer-aware update scheme.

Empirically, across a diverse set of model–dataset pairs spanning MLPs, CNNs, and Transformers, we observe structured layerwise hardness profiles and assess their robustness under different initializations. We further study a deterministic ReLU-ization strategy in which the learned gates are progressively hardened toward a principled target, enabling a post-training substitution of λ -GELU by ReLU with reduced disruption. Overall, λ -GELU provides a minimal and interpretable knob to profile and control gating hardness, bridging smooth training with ReLU-centric downstream pipelines.

Index Terms—Parametric Activation Functions, GELU, Deep Learning Optimization, Learnable Hardness

I. INTRODUCTION

Activation functions shape both the optimization dynamics and the functional form of deep neural networks. Modern practice is largely dominated by rectified nonlinearities such as ReLU [1]–[3], and by smooth, self-gated alternatives (most notably GELU) that have become standard in several Transformer architectures [4]. While smooth gates can be convenient during training, many downstream pipelines in efficient deployment and model analysis are most naturally expressed for piecewise-linear networks and often assume ReLU-type structure (e.g., model compression through pruning and quantization, and piecewise-linear interpretability and verification toolchains) [5]–[8]. This tension motivates mechanisms that

retain the benefits of smooth training recipes while enabling a controlled transition to ReLU-compatible models.

In this work, we study a hardness-parameterized variant of GELU defined as $f(x; \lambda) = x \Phi(\lambda x)$, where Φ is the Gaussian Cumulative Distribution Function (CDF) and $\lambda \in [1, \infty)$ controls the sharpness of the gate. Learning λ is non-trivial and requires a constrained parameterization together with a dedicated optimization scheme to avoid unstable updates and gradient attenuation, which we develop in this paper. Beyond enabling hardness profiling across layers, the learned parameter provides a practical control knob for ReLU-ization: starting after the first 25% of training epochs, we anneal λ toward a large target and evaluate whether the resulting model can be replaced by ReLU with minimal loss in the validation metric.

We emphasize that λ -GELU plays two complementary roles in this work. First, when λ is learned jointly with the weights, it acts as a lightweight probe of layerwise gating hardness, enabling us to characterize consistent hardness hierarchies across architectures and initializations. Second, the same parameter provides a practical control knob for ReLU-ization: once an initial smooth-training phase is completed, λ can be deterministically annealed to enforce ReLU-like gating and enable a clean activation replacement for downstream compatibility or inference deployment.

In summary, our contributions are:

- We introduce λ -GELU as a minimal hardness-controlled family $x \Phi(\lambda x)$ with $\lambda \in [1, \infty)$.
- We develop a stable constrained optimization scheme to learn λ jointly with the network parameters, based on softplus reparameterization and a dedicated learning-rate scaling for this hardness variable.
- We propose a deterministic hardening-and-replacement protocol: after a smooth-training phase, we freeze λ and linearly anneal it toward a principled target λ_{target} , and we evaluate ReLU substitution at the best-validation checkpoint without further weight updates.

*Corresponding author

The remainder of the paper is organized as follows. Section II reviews related work on smooth and parametric activation functions and on ReLU-centric downstream pipelines in compression, interpretability, and verification. Section III introduces the proposed framework and the constrained optimization strategy for learning λ . Section IV reports an empirical evaluation across multiple datasets and architectures and studies the proposed annealing procedure. Finally, Section V concludes and outlines future research directions.

II. RELATED WORK

Rectified activations, and in particular ReLU, mitigate gradient attenuation effects that hinder deep optimization and have become a default choice in many pipelines [1]–[3]. At the same time, their non-differentiability at the origin and issues such as inactive (“dead”) units have motivated a large body of work on smooth alternatives. Representative examples include GELU [4], SiLU [9], Swish [10], and Mish [11]. Many of these can be interpreted as *self-gated* activations of the form $x\phi(x)$, where the gate $\phi(x) \in (0, 1)$ is a smooth approximation to a Heaviside-type decision. In particular, GELU has become prevalent in Transformer-based architectures, where it is frequently adopted as a default activation [4].

A natural extension of both rectifiers and smooth gates is to make the nonlinearity *adaptive* by introducing learnable parameters controlling slope, curvature, saturation, or sharpness. Examples include parametric rectifiers such as PReLU [12] and other variants that learn thresholds or slopes, as well as smooth gates with tunable “temperature”-like parameters. These approaches are motivated by improved optimization and task adaptivity, but they also raise stability concerns: unconstrained parameters may drift to degenerate regimes, and naive parameterizations can lead to vanishing or overly unstable gradients.

The closest formulation to our own is the learnable- β variant of Swish [10], $x \cdot \sigma(\beta x)$, which also introduces a scalar sharpness-like parameter. However, β is unconstrained (it can take negative values, collapsing toward zero), and no annealing protocol toward a piecewise-linear target has been proposed for it. PReLU [12] is also related in that it learns a per-layer scalar, but it modifies the slope of the negative half-plane rather than gating sharpness, and does not converge to ReLU as the parameter grows. Our λ -GELU differs from both in three concrete ways: (i) $\lambda \geq 1$ is enforced by construction, grounding the family at standard GELU; (ii) we derive a principled annealing target λ_{target} from a closed-form ℓ_1 approximation bound between $\Phi(\lambda x)$ and the Heaviside gate; and (iii) we directly evaluate ReLU substitution quality at the end of training. Our work, thus, contributes to this line by explicitly modeling a hardness parameter in a GELU-style gate and by focusing on how to learn it stably under the natural constraint $\lambda \geq 1$ via reparameterization and optimizer-aware scaling.

Beyond training-time considerations, a large ecosystem of deployment and analysis methods is best aligned with

piecewise-linear networks and often implicitly assumes ReLU-type nonlinearities. This is particularly clear in:

Quantization and efficient inference. Integer-only quantization pipelines are most naturally expressed with linear operators and simple piecewise-linear nonlinearities, and classic schemes for quantization-aware training and efficient inference are commonly presented for ReLU-based networks [5]. In contrast, smooth nonlinearities such as GELU require either mixed-precision handling or dedicated approximations to enable efficient integer-only execution. This challenge is explicit in work on quantized Transformers, where GELU is approximated to support integer arithmetic [13].

Pruning and sparsity-driven compression. Many pruning and compression heuristics exploit the exact zeroing behavior induced by rectifiers, enabling criteria based on activation sparsity and facilitating structured removal of units or channels. For instance, Network Trimming leverages the Average Percentage of Zeros (APoZ) after ReLU to identify and prune redundant neurons/feature maps [6]. Such sparsity-based signals are less direct for smooth activations that rarely produce exact zeros, which can reduce both the interpretability of sparsity metrics and potential hardware speedups.

Interpretability and formal analysis for piecewise-linear networks. Several “white-box” interpretability methods are designed around piecewise-linear structure, enabling exact region-wise linear explanations of network behavior. OPEN-BOX, for example, provides exact and consistent interpretability for piecewise-linear neural networks by converting them into equivalent collections of linear models [7]. Similarly, formal verification and robustness analysis toolchains commonly target ReLU networks because ReLU constraints admit efficient reasoning via SAT/SMT-style procedures, linear relaxations, or dedicated solvers. Reluplex [8] and Marabou [14] are representative systems that build on ReLU’s piecewise-linear semantics to verify properties of neural networks.

Motivated by these strands, we study a hardness-parameterized GELU gate that can be learned during training and subsequently annealed to approach ReLU-like behavior. This provides a practical bridge between smooth-gated training (often preferred in modern architectures) and ReLU-compatible downstream pipelines in quantization, pruning, interpretability, and verification.

III. PARAMETRIZED GELU

Let Φ and φ denote the CDF and Probability Density Function (PDF) of the standard normal distribution $\mathcal{N}(0, 1)$. We study a parametric variant of GELU defined as

$$\lambda\text{-GELU}(x) = x\Phi(\lambda x), \quad (1)$$

where $\lambda \geq 1$ controls the sharpness of the gate. Note that the standard GELU is recovered at $\lambda = 1$, since $\text{GELU}(x) = x\Phi(x)$.

The gating term $\Phi(\lambda x)$ becomes increasingly sharp as λ grows. In particular, as $\lambda \rightarrow \infty$ we have $\Phi(\lambda x) \rightarrow 1$ when $x > 0$ and $\Phi(\lambda x) \rightarrow 0$ when $x < 0$. Therefore,

$$\lim_{\lambda \rightarrow \infty} x\Phi(\lambda x) = xH(x) = \text{ReLU}(x) \quad (2)$$

where H denotes the Heaviside step function, with $H(0) = \frac{1}{2}$. Consequently, λ -GELU interpolates between GELU-like smooth gating (small λ) and ReLU-like hard gating (large λ). This parameter λ can be shared globally, per layer, per channel, or per neuron, although in this work we only consider the layerwise scenario (one shared λ_ℓ per activation layer).

Optimizing $\lambda \in [1, \infty)$ directly can be inconvenient for SGD-like methods because unconstrained gradient steps may propose updates that cross below 1. We thus introduce an unconstrained parameter $s \in \mathbb{R}$ and map it to $\lambda > 1$ through a softplus reparameterization:

$$\lambda(s) = 1 + \text{softplus}\left(\frac{s}{t}\right) = 1 + \log(1 + e^{\frac{s}{t}}),$$

where $t > 0$ is a temperature controlling the sensitivity of λ with respect to s . In this work, t is treated as a hyperparameter (not learned). This reparameterization has three practical benefits. First, it converts the constrained optimization problem $\lambda \in [1, \infty)$ into unconstrained updates over $s \in \mathbb{R}$, which is directly compatible with standard SGD-like optimizers. Second, the mapping is smooth and computationally inexpensive, as softplus is optimized in most Deep Learning (DL) frameworks. Third, it makes explicit how the temperature t modulates the sensitivity of λ to gradient-based updates.

Let $\delta := \partial L / \partial a$ denote the backpropagated signal at the activation output $a(x; \lambda) = x\Phi(\lambda x)$. By the chain rule,

$$\frac{\partial L}{\partial s} = \frac{\partial L}{\partial a} \frac{\partial a}{\partial \lambda} \frac{\partial \lambda}{\partial s} = \delta \cdot x^2 \varphi(\lambda x) \cdot \frac{1}{t} \sigma\left(\frac{s}{t}\right),$$

where φ is the standard normal PDF and σ is the sigmoid function. Having $s_{k+1} = s_k - \eta_s \frac{\partial L}{\partial s}$, as the change in s , the induced change in λ can be approximated to first order as

$$\begin{aligned} \Delta \lambda &= \lambda(s_{k+1}) - \lambda(s_k) \approx \frac{\partial \lambda}{\partial s} \Delta s \\ &= -\eta_s \left(\frac{\partial \lambda}{\partial s}\right)^2 \frac{\partial L}{\partial \lambda} = -\eta_s \frac{\sigma(s/t)^2}{t^2} \frac{\partial L}{\partial \lambda}. \end{aligned} \quad (3)$$

Equation (3) highlights two effects. The effective step size on λ scales as $1/t^2$, but it is also *state-dependent* through $\sigma(s/t)$: the same learning rate η_s can translate into very different $\Delta \lambda$ depending on the current value of s . Therefore, changing t is not equivalent to a mere constant rescaling of the learning rate; it also alters the local sensitivity of the mapping $\lambda(s)$ and the magnitude of gradients flowing through s .

To control the adaptation speed of the hardness parameter relative to the network weights, we introduce a learning-rate multiplier. Let η_w denote the learning rate used for the weights, and set $\eta_s = c \cdot \eta_w$, where $c > 0$ is a hyperparameter controlling how aggressively λ adapts compared to the weights. In practice, the effect of this scaling depends on the optimizer: under SGD, c acts as a direct rescaling of the update magnitude, whereas under Adam-like adaptive methods the update is additionally shaped by first- and second-moment estimates, so overly large c may lead to unstable hardness dynamics. In Section IV, we tune (t, c) on a small grid and report stable, best-performing configurations, which we then reuse across the considered model–dataset pairs.

In this work we learn λ layerwise (one hardness parameter per layer), and interpret λ_ℓ as a probe of how decisive the gating should be in layer ℓ : smaller values correspond to smoother transitions, while larger values yield increasingly ReLU-like behavior. Empirically, we first characterize the resulting layerwise hardness profiles across architectures and study their robustness across random initializations.

Motivated by the fact that many downstream pipelines are most naturally expressed for ReLU/piecewise-linear networks, we propose a gradual hardening procedure. Specifically, we train λ -GELU normally for the first 25% of the training epochs and then progressively increase λ according to a prescribed annealing schedule over the remaining epochs. We detail the protocol and report results in Section IV.

IV. EXPERIMENTS

This section reports the empirical results of our approach and evaluates it under different experimental conditions.

As stated above, this work does not aim to introduce a new activation function. Rather, we use the λ -GELU parametrization as a probe to study how gating hardness evolves during training, by tracking the learned sharpness parameter across depth. Accordingly, our experimental goal is not to outperform the baselines in predictive performance, but (i) to characterize and compare the resulting hardness dynamics across architectures and datasets; and (ii) to evaluate a hardening-and-replacement procedure that anneals λ after the first 25% of training epochs and tests whether the resulting model can be replaced by a ReLU network with minimal loss in validation performance.

To this end, we selected a diverse set of models and datasets to cover the main architectural families used in contemporary DL. For each family, we previously perform a hyperparameter sweep over the learning rate (LR) and weight decay (WD) on the baseline model, and report only the configuration achieving the highest validation score. We consider:

- **Multilayer Perceptrons (MLPs):** a 4-layer MLP with 256 hidden units per layer, trained with SGD using LR = $5 \cdot 10^{-2}$ and WD = 10^{-4} .
- **Convolutional Neural Networks (CNNs):** ResNet-18, trained with AdamW using LR = $5 \cdot 10^{-4}$ and WD = 10^{-4} .
- **Transformers:** DeiT (vision) and GPT-2 (language). DeiT is trained with AdamW using LR = $5 \cdot 10^{-4}$ and WD = $7 \cdot 10^{-2}$, while GPT-2 is trained with AdamW using LR = $5 \cdot 10^{-5}$ and WD = 10^{-2} .

We evaluate six model–dataset benchmarks: MLP/Adult [15], MLP/FMNIST [16], ResNet-18 [17]/CIFAR-10 [18], ResNet-18 [17]/CIFAR-100 [18], DeiT (Tiny) [19] /TinyImageNet [20], and GPT-2 [21]/WikiText-2 [22]. All experiments are conducted in Python v3.10 with PyTorch v2.6; we fix 3 random seeds for reproducibility. Metrics are reported as mean \pm standard deviation across the 3 seeds. We use validation accuracy for tabular/vision benchmarks and validation perplexity (lower is better) for GPT-2 on WikiText-2.

Unless stated otherwise, we report averages over 3 fixed random seeds. ‘‘Layerwise’’ hardness means one shared parameter λ_ℓ per layer (one scalar per activation layer). This same λ_ℓ is used by the activation applied to all units in MLP layers, all channels in CNN activation sites, and all neurons in Transformer FFN sublayers. For optimization, the unconstrained parameters s use a separate learning rate $\eta_s = c\eta_w$. These parameters are also excluded from weight decay (only the weights are regularized). Additional implementation details and full configurations are provided in the repository¹.

A. Tuning the reparameterization hyperparameters (t, c)

The first experiment performs a grid search over the softplus temperature t and the multiplier c that scales the learning rate of the unconstrained parameter s (cf. Section III, $\eta_s = c\eta_w$). Concretely, we evaluate

$$(t, c) \in \{0.1, 0.3, 0.6, 0.9\} \times \{1, 3, 6, 9\},$$

using an MLP trained on FMNIST with SGD. We repeat each configuration under three initializations of s and three initialization modes $\mathcal{M} = \{\text{uniform, increasing, decreasing}\}$, which control how s (and thus λ) is initialized across depth. The uniform mode sets the same s in every layer, yielding $\lambda \approx 1$ throughout. The increasing/decreasing modes initialize λ monotonically across layers within the range $[1, 2]$ (from ≈ 1 to ≈ 2 , or vice versa) to test whether the learned hardness allocation is robust to the initial ordering. We restrict this range to stay close to the $\lambda=1$ (GELU) baseline while still inducing distinct depth orderings: larger initial values would partially harden the network from the start and substantially attenuate the learning signal for λ , since $\partial a / \partial \lambda = x^2 \varphi(\lambda x)$ concentrates around $x = 0$ as λ grows, leading to small and potentially high-variance gradients under typical pre-activation scales. For a run identified by random seed r , initialization mode $m \in \mathcal{M}$, temperature t , and multiplier c , let $\lambda_\ell^{(r, m, t, c)}(e)$ denote the learned hardness in layer $\ell \in \{1, \dots, L\}$ at epoch e . We quantify hardness adaptation via the average per-layer drift between consecutive epochs,

$$V_\lambda(r, m, t, c) = \frac{1}{L} \sum_{\ell=1}^L \sum_{e=1}^{T-1} \left| \lambda_\ell^{(r, m, t, c)}(e+1) - \lambda_\ell^{(r, m, t, c)}(e) \right|,$$

and report its cell-average

$$\Delta\lambda(t, c) = \mathbb{E}_r \mathbb{E}_{m \in \mathcal{M}} [V_\lambda(r, m, t, c)].$$

$\Delta\lambda(t, c)$ should be interpreted as a proxy for ‘‘how much hardness adapts’’ under a given (t, c) , rather than as an absolute measure of final gate sharpness or a direct indicator of predictive performance. To assess the latter, we use the best validation score (BVS) reached during training. Let

$$\text{BVS}(r, m, t, c) = \max_{e \in \{1, \dots, T\}} \text{val}^{(r, m, t, c)}(e)$$

denote the best validation score of a run. The mean best validation score for λ -GELU and the GELU baseline are

$$\begin{aligned} \overline{\text{BVS}}_\lambda(t, c) &= \mathbb{E}_r \mathbb{E}_{m \in \mathcal{M}} [\text{BVS}(r, m, t, c)], \\ \overline{\text{BVS}}_{\text{GELU}} &= \mathbb{E}_r [\text{BVS}(r, \text{GELU})], \end{aligned} \quad (4)$$

and the heatmap annotations report their difference,

$$\Delta\text{BVS}(t, c) = \overline{\text{BVS}}_\lambda(t, c) - \overline{\text{BVS}}_{\text{GELU}}.$$

Figure 1 summarizes the grid: the color encodes the mean hardness drift $\Delta\lambda(t, c)$, while the cell annotation shows $\Delta\text{BVS}(t, c)$. Two expected monotonic trends are visible. First, smaller temperatures increase the sensitivity of the mapping $\lambda(s)$, amplifying hardness adaptation. Second, larger c yields larger updates on s , which also increases $\Delta\lambda$. Among the tested temperatures, $t = 0.1$ provides the most favorable trade-off, retaining substantial hardness drift while keeping ΔBVS close to the GELU baseline.

Because scaling η_s under AdamW is not equivalent to a pure gradient rescaling (due to first/second-moment accumulation), we additionally run a reduced proxy (ResNet18 on CIFAR100) sweep for AdamW-based settings: we fix $t = 0.1$ and sweep $c \in \{1, 3, 6, 9\}$. As shown in Figure 2, increasing c again monotonically increases $\Delta\lambda$, while ΔBVS remains small in magnitude across the sweep. Although $c = 1$ achieves the best mean ΔBVS in this proxy, $c = 9$ is comparable while maximizing hardness adaptation.

Overall, across the explored grid, learning λ leaves the best validation score close to the GELU baseline while enabling a controllable amount of hardness adaptation. In our subsequent experiments we fix $t = 0.1$ and $c = 9$ as a simple choice that consistently produced substantial $\Delta\lambda$ without degrading BVS in the considered settings; we do not claim this pair to be universally optimal across all architectures and optimizers.

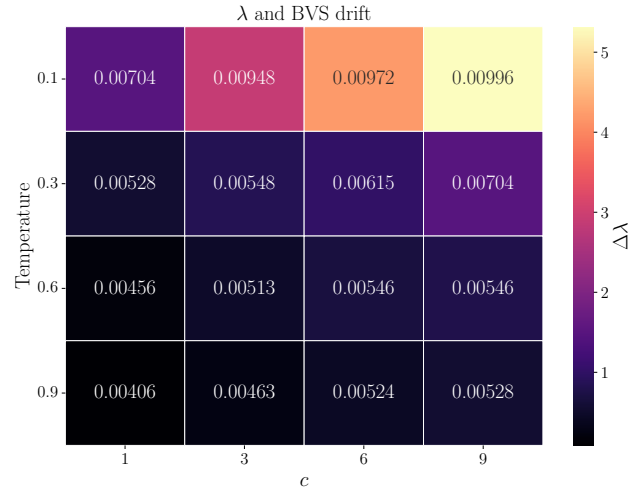


Fig. 1. Grid over temperature t and the s learning-rate multiplier c on MLP/FMNIST. Cell annotations report the mean validation-score change with respect to GELU (averaged over the three s initializations), while the color encodes the mean hardness-drift proxy $\Delta\lambda$ (average absolute epoch-to-epoch change of the learned layerwise hardness). Low temperatures and larger c induce stronger hardness adaptation.

¹All code configurations will be provided upon acceptance

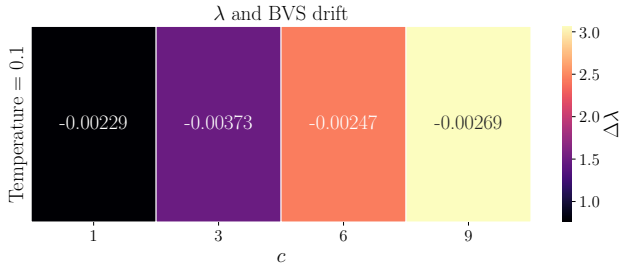


Fig. 2. Sweep over the s learning-rate multiplier c on ResNet-18/CIFAR-100 (AdamW, $t=0.1$ fixed). Cell annotations report the mean validation-score change with respect to GELU (averaged over the three s initializations), while the color encodes the mean hardness-drift proxy $\Delta\lambda$ (average absolute epoch-to-epoch change of the learned layerwise hardness). Larger c monotonically increases $\Delta\lambda$ while ΔBVS remains small across the sweep; $c=1$ achieves the best mean ΔBVS but $c=9$ is comparable while maximizing hardness adaptation.

B. Evaluation of λ -GELU under different initializations

The next experiment evaluates all selected model–dataset pairs and characterizes how the learned layerwise hardness parameters evolve throughout training. For each configuration, we report: (i) the validation-metric trajectory; and (ii) the Spearman rank correlation between the layerwise hardness vectors obtained under different initializations of the parameter s . At each epoch e , we form the layerwise hardness profile $\bar{\lambda}^{(r,m)}(e) \in \mathbb{R}^L$ and compute the Spearman rank correlation between profiles obtained from two s -initialization modes m_1, m_2 :

$$\rho_S(e; m_1, m_2) = \mathbb{E}_r \left[\text{Spearman}(\bar{\lambda}^{(r,m_1)}(e), \bar{\lambda}^{(r,m_2)}(e)) \right].$$

High values of ρ_S indicate that the relative ordering of layers by hardness is preserved across initializations, i.e., layers that become harder under one initialization also tend to be harder under the others (up to a monotone transformation). Therefore, this experiment tests whether training induces an initialization-robust layerwise hardness hierarchy, rather than an initialization-dependent allocation of hardness across depth.

Figure 3 reports validation trajectories (left) and the corresponding Spearman correlations of layerwise hardness rankings across initialization modes (right). Shadow indicates the standard deviation across seeds. Several vision settings (MLP on FMNIST, ResNet-18 on CIFAR-10/100, and DeiT on TinyImageNet) converge to consistently high ρ_S , indicating that training induces an initialization-robust ordering of layers by hardness.

In contrast, for Adult and especially for GPT-2/WikiText-2, ρ_S is lower and/or stabilizes later, suggesting that under our fixed (t, c) the allocation of hardness across depth is more sensitive to initialization and optimizer dynamics. This points to the need for architecture-specific tuning of hardness learning (or longer training) to obtain robust layerwise profiles in these regimes.

These results are also summarized in Table I Here, BVS denotes the best validation score achieved during training; validation accuracy for all vision/tabular benchmarks, and

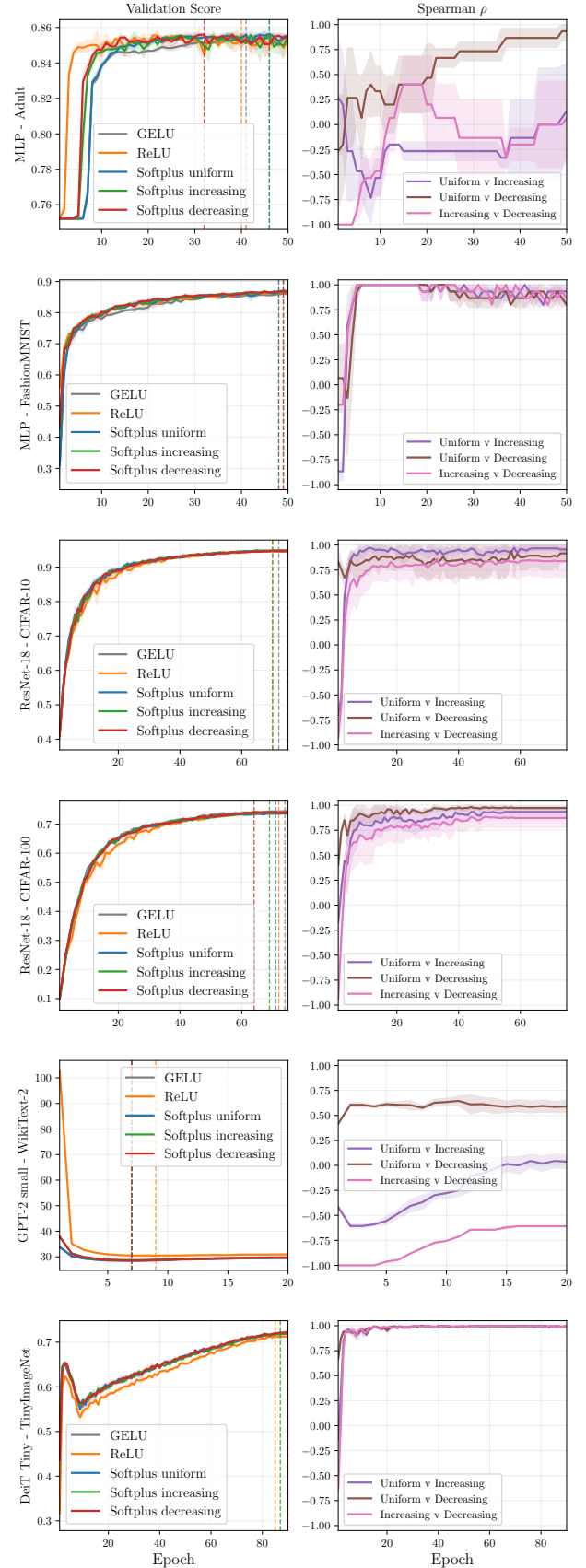


Fig. 3. Validation-metric trajectories (left) and Spearman rank correlations between layerwise hardness profiles across s -initialization modes (right). Vertical lines mark the epoch of best validation score (BVS).

validation perplexity for GPT-2 on WikiText-2 (lower is better). Ep. is the epoch at which BVS is reached. $\bar{\lambda}$ is the network-wide mean of the learned layerwise hardness values, and $\overline{\Delta\lambda}$ is the corresponding mean drift across seeds and layers. A mild trend can be observed: architectures that are more commonly trained with ReLU (e.g., the MLP and CNN considered here) tend to learn larger average values of λ than architectures typically trained with GELU. We interpret this as a possible indication of a preference toward harder gating in those settings under our training configuration, rather than as a universal property.

Overall, Table I shows that the baseline and the different λ -GELU initialization modes achieve similar best validation scores in most benchmarks, with differences that are generally small. In our experiments, the uniform initialization is a reasonable default choice: it performs comparably to the increasing/decreasing schemes while remaining initialization-neutral and adding only one learnable hardness parameter per activation layer, which is negligible relative to the total number of network parameters.

TABLE I
SUMMARY OF THE METRICS REPORTED IN OUR EXPERIMENTS
(IDENTIFIED BY DATASET).

Dataset	Act.	Mode	BVS	Ep.	$\bar{\lambda}$	$\overline{\Delta\lambda}$
Adult	GELU	-	$0.85 \pm 4 \cdot 10^{-4}$	41	-	-
		ReLU	$0.86 \pm 6 \cdot 10^{-4}$	40	-	-
	λ -GELU	dec	$0.87 \pm 8 \cdot 10^{-4}$	32	6.66 ± 0.13	8.10 ± 0.2
		inc	$0.86 \pm 9 \cdot 10^{-4}$	46	8.67 ± 0.10	11.63 ± 0.49
		uni	0.86 ± 10^{-3}	46	2.45 ± 0.07	3.23 ± 0.49
FMNIST	GELU	-	$0.86 \pm 2 \cdot 10^{-3}$	49	-	-
		ReLU	$0.86 \pm 1 \cdot 10^{-3}$	48	-	-
	λ -GELU	dec	$0.87 \pm 3 \cdot 10^{-3}$	49	$3.40 \pm 3 \cdot 10^{-2}$	6.34 ± 0.17
		inc	$0.87 \pm 2 \cdot 10^{-3}$	50	$3.41 \pm 3 \cdot 10^{-2}$	6.85 ± 0.14
		uni	$0.87 \pm 8 \cdot 10^{-4}$	48	$3.09 \pm 2 \cdot 10^{-2}$	6.48 ± 0.17
CIFAR10	GELU	-	$0.95 \pm 1 \cdot 10^{-3}$	72	-	-
		ReLU	$0.95 \pm 1 \cdot 10^{-3}$	70	-	-
	λ -GELU	dec	$0.95 \pm 2 \cdot 10^{-3}$	75	$2.43 \pm 6 \cdot 10^{-2}$	4.55 ± 0.15
		inc	$0.95 \pm 4 \cdot 10^{-4}$	70	1.68 ± 0.39	3.51 ± 0.76
		uni	$0.95 \pm 6 \cdot 10^{-4}$	75	1.75 ± 0.51	3.22 ± 0.61
CIFAR100	GELU	-	$0.74 \pm 5 \cdot 10^{-3}$	74	-	-
		ReLU	$0.73 \pm 3 \cdot 10^{-3}$	72	-	-
	λ -GELU	dec	$0.74 \pm 3 \cdot 10^{-3}$	64	$2.64 \pm 9 \cdot 10^{-2}$	4.23 ± 0.13
		inc	$0.74 \pm 3 \cdot 10^{-3}$	69	1.65 ± 0.48	3.18 ± 0.77
		uni	$0.74 \pm 3 \cdot 10^{-3}$	71	1.89 ± 0.39	3.39 ± 0.60
TinyImageNet	GELU	-	$0.72 \pm 1 \cdot 10^{-3}$	90	-	-
		ReLU	$0.71 \pm 8 \cdot 10^{-4}$	85	-	-
	λ -GELU	dec	$0.72 \pm 2 \cdot 10^{-3}$	90	$1.21 \pm 1 \cdot 10^{-3}$	$1.39 \pm 2 \cdot 10^{-2}$
		inc	$0.72 \pm 2 \cdot 10^{-3}$	87	$1.21 \pm 1 \cdot 10^{-3}$	$1.43 \pm 4 \cdot 10^{-2}$
		uni	$0.72 \pm 1 \cdot 10^{-4}$	90	$1.19 \pm 2 \cdot 10^{-4}$	$1.36 \pm 3 \cdot 10^{-2}$
WikiText-2	GELU	-	$28.46 \pm 2 \cdot 10^{-2}$	7	-	-
		ReLU	$30.48 \pm 4 \cdot 10^{-2}$	9	-	-
	λ -GELU	dec	$28.59 \pm 9 \cdot 10^{-3}$	7	$1.24 \pm 6 \cdot 10^{-5}$	$0.28 \pm 2 \cdot 10^{-4}$
		inc	$28.71 \pm 2 \cdot 10^{-2}$	7	$1.24 \pm 1 \cdot 10^{-4}$	$0.29 \pm 2 \cdot 10^{-5}$
		uni	$28.45 \pm 2 \cdot 10^{-2}$	7	$1.00 \pm 8 \cdot 10^{-6}$	$2 \cdot 10^{-3} \pm 1 \cdot 10^{-5}$

C. Hardness annealing and ReLU replacement

A practical motivation for learning gating hardness is to enable a *controlled* conversion from GELU-based training to a ReLU-compatible model at the end of training. Rather than

retraining a ReLU network from scratch or performing a hard swap mid-training (which may introduce an abrupt distributional shift), we aim to progressively sharpen the learned gates. This way, the resulting network approaches piecewise-linear behavior and becomes amenable to downstream pipelines that assume ReLU/piecewise-linear structure (e.g., quantization, sparsity-driven compression, and analysis toolchains).

In this experiment, we propose a gradual hardening procedure followed by a post-training activation substitution test. We train λ -GELU normally for the first 25% of epochs, and then enforce a deterministic hardening schedule. We set the switch point to 25% of training as a reasonable fixed baseline that preserves an initial smooth-gating phase while leaving sufficient training time for the network to adapt to the progressive hardening. Switching too early (e.g., 10%) shortens the smooth-gating phase and may underuse the optimization benefits of GELU-like curvature, whereas switching too late (e.g., 50%) may increase the abruptness of the distribution shift induced by hardening. Using a fixed 25% switch across all benchmarks also avoids per-dataset tuning and provides a consistent evaluation protocol. To evaluate replacement, we select the checkpoint corresponding to the best validation epoch (under the original activation or annealed one), and at that checkpoint we measure: (i) the validation metric with the original activation; and (ii) the validation metric after substituting GELU/ λ -GELU by ReLU, without any further weight updates and on the same validation split.

Algorithm 1 Deterministic hardening and ReLU substitution

- 1: Train λ -GELU with learnable $\{s_\ell\}_{\ell=1}^L$ for $e = 1, \dots, e_s = \lfloor 0.25T \rfloor$.
- 2: Save the learned hardness values $\{\lambda_\ell(e_s)\}_{\ell=1}^L$.
- 3: **for** $e = e_s + 1, \dots, T$ **do**
- 4: Set $\lambda_\ell(e) \leftarrow \lambda_\ell(e_s) + \frac{e - e_s}{T - e_s} (\lambda_{\text{target}} - \lambda_\ell(e_s))$ for all ℓ .
- 5: Freeze s (no gradient updates) and continue training weights.
- 6: **end for**
- 7: Select the best-validation checkpoint (under λ -GELU).
- 8: Evaluate validation metric with λ -GELU; then substitute activations by ReLU and re-evaluate.

In all annealing runs, the schedule enforces $\lambda_\ell(T) = \lambda_{\text{target}}$ for every layer ℓ , ensuring that the final gates are uniformly hardened before the substitution test. To clarify the annealing process, we present it as pseudocode in Algorithm 1. Note that during hardening, λ is not learnable: we stop gradient updates for s and override λ with a deterministic linear schedule toward λ_{target} over the remaining 75% of training. Algorithm 1 summarizes the procedure. To set the annealing target λ_{target} in a principled way, we quantify how well the smooth gate $\Phi(\lambda x)$ approximates the hard gate $H(x)$ as a function of λ . A closed-form computation yields the global bound

$$E_\infty(\lambda) = \int_{-\infty}^{\infty} |H(x) - \Phi(\lambda x)| dx = \frac{2}{\lambda\sqrt{2\pi}}.$$

Therefore, given a tolerance $\varepsilon > 0$, it suffices to choose $\lambda_{\text{target}} \geq \frac{2}{\varepsilon\sqrt{2\pi}}$; in particular, $\varepsilon = 5 \times 10^{-3}$ gives $\lambda_{\text{target}} \approx 160$. In the experiments below, we use this criterion to select λ_{target} for annealing, and we report results across all model–dataset benchmarks by comparing the GELU baseline and the λ -GELU with post-25% hardness annealing toward λ_{target} .

We use $E_{\infty}(\lambda)$ to choose λ_{target} because it is distribution-agnostic: it depends only on the gate family and the desired tolerance, and it does not require estimating pre-activation statistics that vary across architectures due to normalization (e.g., batch/layer normalization) and training dynamics. This makes λ_{target} a conservative but generic choice that can be reused across all model–dataset pairs.

We report annealing-and-substitution results for the tabular and vision benchmarks. For GPT-2/WikiText-2, activation substitution remains unstable under our protocol (see discussion below), so we omit it from Table II. Table II reports these experiments, where the λ -GELU has been annealed. In particular, we select the checkpoint at the best validation epoch under the original activation (GELU or λ -GELU). “Original” reports the validation metric at that checkpoint; “Substituted” reports the validation metric after replacing the activation by ReLU at the same checkpoint, without further weight updates (mean over 3 seeds). Overall, ReLU-ization preserves the validation metric substantially better when it is preceded by our annealing procedure: by progressively increasing λ , the network adapts to harder gating during training, so that the subsequent replacement of λ -GELU by ReLU induces only a minor change in the effective input–output mapping. Across the tabular and vision benchmarks, the annealed replacement consistently reduces the performance drop relative to a direct GELU→ReLU swap, and in some cases it even matches (or slightly improves upon) the pre-replacement score (e.g., Adult). In contrast, directly swapping GELU for ReLU without prior hardening typically causes a noticeable degradation, consistent with an abrupt distributional shift in intermediate activations.

Transformer training is markedly more sensitive to activation replacement. For GPT-2 on WikiText-2 (where the validation metric is perplexity, lower is better), replacing GELU with ReLU causes a severe deterioration in both the GELU and λ -GELU cases, suggesting that additional mechanisms (e.g., post-swap fine-tuning or architecture-specific hardening strategies) are required for language modeling; therefore, we do not report those results here and we leave this analysis for future work.

For Table II, “Original” refers to the validation metric at the selected best-validation checkpoint under the activation used in each row: the GELU checkpoint for the GELU baseline, and the annealed λ -GELU checkpoint for the λ -GELU row.

V. CONCLUSION AND FUTURE DIRECTIONS

We introduced λ -GELU, a hardness-parameterized variant of GELU of the form $x\Phi(\lambda x)$ with $\lambda \geq 1$, and used it as a lightweight probe to study and control gating hardness in deep networks. To enable stable learning of λ ,

TABLE II
ANNEALING AND REPLACEMENT EVALUATION ON THE VALIDATION SET.

Dataset	Mode	Original metric	Substituted metric
Adult	GELU	0.85	0.80
	λ -GELU	0.81	0.81
FMNIST	GELU	0.86	0.83
	λ -GELU	0.86	0.85
CIFAR10	GELU	0.95	0.92
	λ -GELU	0.95	0.95
CIFAR100	GELU	0.74	0.67
	λ -GELU	0.74	0.72
TinyImageNet	GELU	0.71	0.68
	λ -GELU	0.71	0.72

we proposed a constrained optimization scheme based on a temperature-controlled softplus reparameterization, and a dedicated learning-rate multiplier for the unconstrained hardness variable. Across a grid search over (t, c) , we found that hardness adaptation can be made substantial while keeping the best validation score close to the GELU baseline.

Across six model–dataset benchmarks spanning different models (MLP, ResNet-18, DeiT, and GPT-2), we observed structured layerwise hardness dynamics and evaluated their robustness to different initializations through Spearman rank correlation. In several vision and tabular settings, the relative ordering of layers by hardness becomes consistent across initializations, suggesting that training induces a repeatable hardness allocation across depth. Finally, we proposed a gradual ReLU-ization procedure: after an empirically selected switch point at 25% of training epochs, we anneal λ toward a target λ_{target} chosen from an ℓ_1 approximation bound between $\Phi(\lambda x)$ and the Heaviside gate. The resulting hardened models can be replaced by ReLU with substantially smaller degradation than a direct GELU→ReLU swap, and in some cases the replacement matches the pre-swap validation metric. Transformer activation replacement remains challenging: while annealing mitigates the shock relative to a direct swap, it does not fully preserve performance in language modeling. We view this as a first step that motivates future work on architecture-aware hardening and replacement criteria in the presence of residual connections and normalization. Our choice of λ_{target} is intentionally distribution-agnostic: it guarantees a uniform gate-approximation tolerance independently of the pre-activation statistics, at the cost of being conservative for normalized architectures. A tighter alternative would set layer-specific targets from empirical pre-activation distributions; we leave this refinement for future work.

This work provides a minimal and practical bridge between smooth-gated training and ReLU-compatible models. Future work includes extending hardness learning to other self-gated activations, exploring finer granularities (per-channel or per-neuron hardness), and developing adaptive schedules

for the annealing onset and rate. A particularly important direction is to quantify downstream benefits in the settings that motivate ReLU-ization, such as integer-only quantization, sparsity-based compression, and piecewise-linear analysis and verification pipelines.

Finally, while we motivate ReLU-ization by compatibility with piecewise-linear deployment and analysis pipelines, a systematic evaluation of downstream gains (e.g., integer-only quantization, sparsity-driven pruning, and verification/interpretability toolchains) is an important next step beyond the scope of this submission.

ACKNOWLEDGMENT

This research was funded by the projects PID2023-146569NB-C21 and PID2023-146569NB-C22 supported by MICIU/AEI/10.13039/501100011033 and ERDF/UE. Cristian Pérez-Corral received support from the *Conselleria de Educaci3n, Cultura, Universidades y Empleo* (reference CIACIF/2024/412) through the European Social Fund Plus 2021–2027 (FSE+) program of the *Comunitat Valenciana*. Alberto Fern3ndez-Hern3ndez was supported by the predoctoral grant PREP2023-001826 supported by MICIU/AEI/10.13039/501100011033 and ESF+. Jose I. Mestre was supported by the predoctoral grant ACIF/2021/281 of the *Generalitat Valenciana*. Manuel F. Dolz was supported by the Plan Gen–T grant CIDEXG/2022/13 of the *Generalitat Valenciana*.

REFERENCES

- [1] V. Nair and G. E. Hinton, “Rectified linear units improve restricted boltzmann machines,” in *Proceedings of the 27th International Conference on International Conference on Machine Learning*, ser. ICML’10. Madison, WI, USA: Omnipress, 2010.
- [2] X. Glorot, A. Bordes, and Y. Bengio, “Deep sparse rectifier neural networks,” in *Proceedings of the Fourteenth International Conference on Artificial Intelligence and Statistics*, ser. Proceedings of Machine Learning Research. PMLR, 2011.
- [3] A. Krizhevsky, I. Sutskever, and G. E. Hinton, “Imagenet classification with deep convolutional neural networks,” in *Advances in Neural Information Processing Systems 25: 26th Annual Conference on Neural Information Processing Systems 2012*, P. L. Bartlett, F. C. N. Pereira, C. J. C. Burges, L. Bottou, and K. Q. Weinberger, Eds., 2012.
- [4] D. Hendrycks and K. Gimpel, “Gaussian error linear units (gelus),” *arXiv preprint arXiv:1606.08415*, 2016.
- [5] B. Jacob, S. Kligys, B. Chen, M. Zhu, M. Tang, A. Howard, H. Adam, and D. Kalenichenko, “Quantization and training of neural networks for efficient integer-arithmetic-only inference,” in *Proceedings of the IEEE Conference on Computer Vision and Pattern Recognition (CVPR)*, June 2018.
- [6] H. Hu, R. Peng, Y. Tai, and C. Tang, “Network trimming: A data-driven neuron pruning approach towards efficient deep architectures,” *CoRR*, vol. abs/1607.03250, 2016.
- [7] L. Chu, X. Hu, J. Hu, L. Wang, and J. Pei, “Exact and consistent interpretation for piecewise linear neural networks: A closed form solution,” in *Proceedings of the 24th ACM SIGKDD International Conference on Knowledge Discovery & Data Mining*, ser. KDD ’18, 2018.
- [8] G. Katz, C. W. Barrett, D. L. Dill, K. Julian, and M. J. Kochenderfer, “Reluplex: An efficient SMT solver for verifying deep neural networks,” *CoRR*, vol. abs/1702.01135, 2017.
- [9] S. Elfving, E. Uchibe, and K. Doya, “Sigmoid-weighted linear units for neural network function approximation in reinforcement learning,” *arXiv preprint*, 2017.
- [10] P. Ramachandran, B. Zoph, and Q. V. Le, “Searching for activation functions,” 2017.
- [11] D. Misra, “Mish: A self regularized non-monotonic activation function,” 2020.
- [12] K. He, X. Zhang, S. Ren, and J. Sun, “Delving deep into rectifiers: Surpassing human-level performance on imagenet classification,” in *Proceedings of the IEEE international conference on computer vision*, 2015, pp. 1026–1034.
- [13] S. Kim, A. Gholami, Z. Yao, M. W. Mahoney, and K. Keutzer, “I-bert: Integer-only bert quantization,” *International Conference on Machine Learning*, 2021.
- [14] G. Katz, D. Huang, D. Ibeling, K. Julian, C. Lazarus, R. Lim, P. Shah, S. Thakoor, H. Wu, A. Zeljić, D. Dill, M. Kochenderfer, and C. Barrett, “The marabou framework for verification and analysis of deep neural networks,” in *Computer Aided Verification*, 2019.
- [15] B. Becker and R. Kohavi, “Adult,” UCI Machine Learning Repository, 1996, DOI: <https://doi.org/10.24432/C5XW20>.
- [16] H. Xiao, K. Rasul, and R. Vollgraf, “Fashion-mnist: a novel image dataset for benchmarking machine learning algorithms,” 2017.
- [17] K. He, X. Zhang, S. Ren, and J. Sun, “Deep residual learning for image recognition,” in *2016 IEEE Conference on Computer Vision and Pattern Recognition (CVPR)*, 2016.
- [18] A. Krizhevsky, “Learning multiple layers of features from tiny images,” *University of Toronto*, 05 2012.
- [19] H. Touvron, M. Cord, M. Douze, F. Massa, A. Sablayrolles, and H. Jégou, “Training data-efficient image transformers & distillation through attention,” 2021.
- [20] Y. Le and X. S. Yang, “Tiny imagenet visual recognition challenge,” 2015.
- [21] A. Radford, J. Wu, R. Child, D. Luan, D. Amodei, and I. Sutskever, “Language models are unsupervised multitask learners,” *OpenAI*, 2019.
- [22] S. Merity, C. Xiong, J. Bradbury, and R. Socher, “Pointer sentinel mixture models,” in *International Conference on Learning Representations*, 2017.